Article

The Contribution of the Corpus Callosum to the Symmetrical Representation of Taste in the Human Brain: An fMRI Study of Callosotomized Patients

Gabriele Polonara [1] , Giulia Mascioli [1,†], Ugo Salvolini [1,‡], Aldo Paggi [2,‡], Tullio Manzoni [3,§] and Mara Fabri [4,*]

1   Dipartimento di Scienze Cliniche Specialistiche e Odontostomatologiche, Università Politecnica delle Marche, 60020 Ancona, Italy; g.polonara@staff.univpm.it (G.P.); giuliamascioli5@gmail.com (G.M.); u.salvolini@gmail.com (U.S.)
2   Centro Epilessia, Ospedale Regionale Umberto I, 60020 Ancona, Italy; aldopaggi@libero.it
3   Dipartimento di Medicina Sperimentale e Clinica, Università Politecnica delle Marche, 60020 Ancona, Italy
4   Dipartimento di Scienze della Vita e dell'Ambiente, Università Politecnica delle Marche, 60131 Ancona, Italy
*   Correspondence: m.fabri@staff.univpm.it
†   Current address: General Medicine Doctor, Via Bixio 99, 60015 Falconara, Italy.
‡   Off duty Professor.
§   Deceased.

Abstract: The present study was designed to establish the contribution of the corpus callosum (CC) to the cortical representation of unilateral taste stimuli in the human primary gustatory area (GI). Unilateral taste stimulation of the tongue was applied to eight patients with partial or total callosal resection by placing a small cotton pad soaked in a salty solution on either side of the tongue. Functional images were acquired with a 1.5 Tesla machine. Diffusion tensor imaging and tractography were also performed. Unilateral taste stimuli evoked bilateral activation of the GI area in all patients, including those with total resection of the CC, with a prevalence in the ipsilateral hemisphere to the stimulated tongue side. Bilateral activation was also observed in the primary somatic sensory cortex (SI) in most patients, which was more intense in the contralateral SI. This report confirms previous functional studies carried out in control subjects and neuropsychological findings in callosotomized patients, showing that gustatory pathways from tongue to cortex are bilaterally distributed, with an ipsilateral predominance. It has been shown that the CC does play a role, although not an exclusive one, in the bilateral symmetrical representation of gustatory sensitivity in the GI area, at least for afferents from one side of the tongue.

Keywords: gustatory stimulation; fMRI; bilateral activation; tongue representation; corpus callosum

1. Introduction

The sense of taste arises mainly from the tongue, where many receptors inform the brain about the nature of the oral content and its suitability for nutrition. Inputs from taste and somatosensory receptors of the tongue signal the molecular composition, texture and temperature of foods and beverages. The taste and somatosensory inputs from the tongue travel to the brain by two separate pathways, the first by the facial and glossopharyngeal nerves and the second by the trigeminal nerve, although the first two nerves may also convey somatosensory information. All these nerves project to the nucleus of the solitary tract (NST), in part on the same neurons [1]. In primates, taste afferents from the NST reach the parvicellular portion (gustatory) of the thalamic ventroposteromedial nucleus (VPMpc) without a relay in the pons [1,2]. Projecting fibers from the thalamus to the cortex gives rise to the somatosensory and gustatory representations of the tongue, also integrating both modalities, in cortical regions of the parietal, frontal and insular lobes [1–5]. In the human brain, the main primary somatosensory representations (SI area) of the tongue lie in the inner and inferior portion of the perirolandic region of the parietal opercula [2–7], whereas

the main primary taste cortical representation (GI area) is in the middle-anterior insula, extending also to the frontal opercula [8–12].

Recent papers investigated the pattern of taste and somatosensory projections from the tongue to the ipsilateral or contralateral hemisphere in humans. Most studies agree that both sides of the tongue are represented in the cortex of the two hemispheres, both in the gustatory and the somatosensory modalities [3,12–18], with a predominant ipsilateral representation in the taste modality and a predominant contralateral representation in the somatosensory modality [3,19,20].

Different sides of the tongue seem to subserve slightly different functions, as recently reported [18]: discrimination is better when tastes are applied to the right tip of the tongue, and the quality is better evaluated when tastes are applied to the left tongue tip. Further, it was found that lesions to both sides of the insula cause bilateral alteration in discrimination, quality evaluation and naming of tastants. Based on these observations and on previous work by others [16,17,20–22], Stevenson et al. [18], and later Iannilli and Gudziol [23], have sketched four/six possible models to explain the transfer of gustatory information from each side of the tongue to the GI area of the ipsilateral and contralateral hemisphere. One of these models [22] suggested the possibility that the corpus callosum (CC) is the only site of the interhemispheric transfer of taste information. However, this hypothesis cannot completely explain the finding that callosotomized patients are able to name basic tastants applied to the right tongue, although their responses are abnormally slow [14,15]. The observation can be explained by hypothesizing that when the CC is lacking, extra time is needed to decode in the left hemisphere (language-dominant) the taste information coming from the right hemitongue via the crossed ascending pathway, which is comparatively weak. Usually, the weaker input from the right side of the tongue to the left hemisphere would be enhanced by input transmitted to the left hemisphere from the right via the CC; the commissure, which can thus be considered as an equalizer, would balance the effects of the ipsilateral and contralateral input, being prevailing the first, and less powerful the second, allowing each hemisphere to receive signals of similar intensity from each side of the tongue [14,15], and thus making the taste representation symmetrical between the two hemispheres.

In a previous study [24], the cortical activation evoked during a taste test like the taste strips [25] was recorded with fMRI. Salt, a basic taste stimulus, was applied along with a tactile stimulus to either side of the tongue; the evoked cortical activation was compared with that evoked by a water stimulus, considered either as a neutral stimulus or a different taste. The results confirmed that a combined taste and somatosensory stimulation of either hemitongue provoked the activation in both hemispheres of cortical areas involved in the primary processing of gustatory modality, i.e., the frontal (FO) and parietal opercula (PO) and the anterior (AI) and middle insula [1,2,17,26–28].

It was also found in most participants that either right or left hemitongue stimulation evoked a bilateral activation of the lower region of the postcentral gyrus in the parietal lobe, which contains the tactile representation of the tongue in the primary somatosensory cortex (SI) [24], in agreement with previous reports [3–6,29,30]. The activations found in the SI area were bilateral, both after right or left hemitongue stimulation and when it was performed with salt or water [24].

However, the origin of bilateral activation of GI areas still remains unsolved. The present study was thus designed to test whether the bilateral activations in the GI area originate from callosal and/or extracallosal pathways since different mechanisms may underpin the bilateral cortical representation of the gustatory system. The research was carried out in eight patients with surgical resection of the CC performed to control drug-resistant epilepsy. In these patients, at least in those in whom the callosal resection involved the anterior third of the commissure, it could be assumed that the callosal contribution to the bilateral representation has been removed, thus making it possible to assess an eventual extracallosal contribution. The cortical activation elicited by unilateral salty stimulation of the tongue was studied and analyzed by fMRI. All patients were also investigated with

diffusion tensor imaging (DTI), a technique designed for the advanced analysis of MR images acquired with diffusion tensor imaging, which permits the depiction of areas of high fractional anisotropy to be displayed in three dimensions. The combination of the two techniques, fMRI and DTI, is a useful method to further validate results.

Some of these results have been presented in preliminary reports [31,32].

2. Methods

2.1. Participants

Eight callosotomized patients (aged 26 to 51 years; mean 35.6 ± 9.3; median 33.5; 25° percentile 2.2; 75° percentile 39; 2 women; Table 1) provided their informed consent to participate in this study. This study was conducted in accordance with the Declaration of Helsinki, and the protocol was approved by the Ethical Committee of Università Politecnica delle Marche (protocol code 200446, date of approval 24 July 2000). The patients, carrying complete or partial surgical resection of the CC to minimize the spread of epileptic seizures (Figure 1), were studied 2 to 21 years from callosotomy. Patients were identified with the same anonymous codes used in a previous paper [33] to allow for the comparison of data from the same patients in different studies. Midsagittal MRI brain images showed that the resection is complete in 3 patients (Figure 1, P2, P3, P5), partial posterior in 1 (Figure 1, P7), partial anterior in 3 patients, either leaving intact only the splenium (Figure 1, P9) or the splenium and the posterior callosal body (Figure 1, P11 and P12), and central in 1 patient (Figure 1, P18). Details of patients' clinical histories and extent of their callosal resection have been reported previously [34,35]. All subjects but one were right-handed, as determined by the Edinburgh handedness inventory [36]. Their postoperative WAIS scores (IQ performance) ranged from 70 to 88 (Table 1). The studies were carried out between 2006 and 2015.

Table 1. Characteristics of patients and types of stimulation administered.

Patient	Gender	Age	I.Q.	Oldfield Score	Callosal Resection	Years from Surgery	DTI	Stimulus Side	Stimulation Protocol
P2	M	51	81	10 (right)	total	21	yes	L, R	p2
P3	M	30	83	21 (right)	total	11	yes	L, R	p2
P5	F	27	70	10 (right)	total	10	yes	L, R	p1
P7	M	48	88	10 (right)	partial posterior	7	yes	L, R	p2
P9	M	35	70	46 (left)	partial anterior	16	yes	L, R	p1
P11	M	36	70	10 (right)	partial anterior	15	yes	L, R	p2
P12	F	32	70	12 (right)	partial anterior	17	yes	L, R	p2
P18	M	26	na	10 (right)	partial central	2	yes	R	p2

L: left; R: right; p1: protocol 1, composed as follows: 60 s rest, 30 s stim, 90 s rest, 30 s stim, 90 s rest; p2: protocol 2, composed as follows: 30 s rest, 15 s stim, 45 s rest, 15 s stim, 45 s rest, 15 s stim, 45 s rest, 15 s stim, 45 s rest, 15 s stim, 15 s rest; na: not available.

Data from patients were compared with data collected in a previous work [24] from a group of healthy subjects composed of 11 volunteers aged 23 to 38 years (mean 28.7 ± 4.3; 7 women; 2 left-handed; median 26; 25° percentile 26; 75° percentile 30.5).

2.2. Imaging Protocols

Functional MRI. Subjects were positioned in a 1.5 Tesla scanner equipped with 50 mT/m gradients (Signa LX NV/©, General Electric Medical System, Milwaukee, WI, USA), with their head restrained in a circularly polarized head coil. They were instructed to keep their eyes closed, hold their tongue out of their mouth, find a comfortable position and relax and avoid even minimal movement; their ears were plugged.
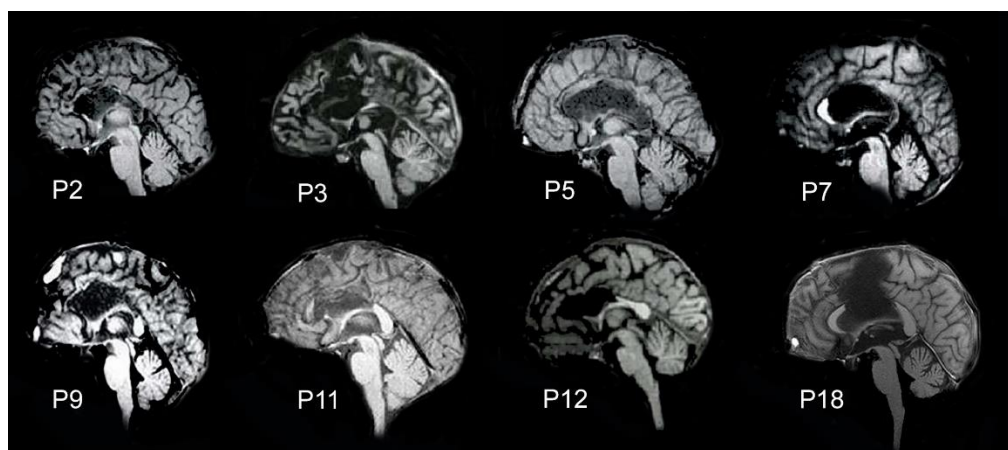
Figure 1. Midsagittal image showing the extent of callosal resection in the 8 patients, showing total callosal resection in 3 patients (P2, P3, P5), partial posterior resection in 1 patient (P7), partial anterior resection sparing the splenium only (P9), the splenium and the callosal body (P11, P12) and partial central resection (P18).

The experimental procedure for fMRI consisted of four steps. In the first, an anatomical sagittal localizer was acquired, and the section levels were selected, from which 10 contiguous 5 mm thick axial sections were later acquired in the third step (see below). The second step involved the acquisition of a 3D data set (IR Prep Fast SPGR 3-D; TR 15.2 ms, TE 6.9 ms, TI 500 ms, Flip Angle 15 degrees, FOV 29 × 29 cm, slice thickness 1 mm, matrix 288 × 288, 1 Nex, and scan time 8:20 min). During the third step axial anatomical images were acquired (T1 FLAIR, 2D, TR 1700 ms, TE 24 ms, Field of View 24 × 24 cm, thickness 5 mm, Matrix 256 × 256, 1 Nex, scan time 2:25 min for 10 images) on which the functional images were overimposed. The fourth step consisted of the fMRI acquisitions in the same 10 axial planes with single-shot T2*-weighted gradient-echo EPI sequences (TR 3000 ms, TE 60 ms, Flip Angle 90°, Field of View 24 × 24 cm, Matrix 64 × 64, 1 Nex, scan time 5:12 min) to obtain images; during the stimulation cycle, 1000 axial functional images in total were acquired simultaneously from the 10 contiguous 5 mm thick axial planes selected under step 1 (100 images/plane, 10 planes, 1 acquisition/3 s, 10 simultaneous images/acquisition). Consecutive images from each section were examined in cine mode to check head movements (see [37] for a review), in which case they were discarded. To obtain the functional images, the blood oxygenation level-dependent (BOLD) contrast method was used.

Diffusion Tensor Imaging. The diffusion tensor MRI and tractography were used in all patients to study connections between the cerebral hemispheres and to compare the data with the results obtained from tractography in normal subjects. For this purpose, 10 oblique axial images were obtained by means of a single-shot spin-echo echo-planar sequence with a diffusion-sensitizing gradient. Diffusion was measured along 25 non-collinear directions. The b-value was 1000 s/mm^2. For the acquisition, the following parameters were selected: TR 6500 ms, TE 76.2 ms, Matrix 128 × 128, FOV 26 × 26 cm, slice thickness 5 mm, interslice gap 1.0 mm, Nex 2, scan time 5:51 min. With these acquisition parameters, the CC was visible through six axial images.

2.3. Gustatory Stimulation

Stimulation was performed by means of a soft cotton pad (3–5 mm tip diameter) soaked in 1M NaCl solution placed on either margin of the protruded tongue at 2.5 cm from the tip. As shown in previous work [14,15], this method ensured that the salty solution remained lateralized to the application side. To avoid influence of meal on the salty perception, participants were asked to abstain from food and beverages, except water, and not to brush their teeth for at least one hour prior to exam. Participants were instructed to protrude their tongue and keep it stable by gently pressing it between the lips for 5 min.

Rinses were avoided to keep the head and the tongue exactly in the same position during the administration of the stimulus to the left or right side of the tongue. An experimenter inside the scanner placed and removed the stimulus pad at appropriate times, according to the block-designed protocol pattern. The cotton pad was attached to a glass pipette 40 cm long so that the experimenter could apply the pad to the chosen tongue location. The experimenter performed stimulations of both sides of the tongue, standing on the left side of the participant, to avoid time waste and participant distraction. The stimulus was always first applied to the left tongue to follow a routine stereotyped sequence for the time and stimulation locus precise control. Two versions of an on–off block-designed stimulation paradigm were used. The first version lasted 5 min and was composed of an initial 60 s rest, followed by two 30 s stimulus-on periods, each followed by 90 s rest periods (protocol n. 1; applied to patients P5 and P9; Figure 2; Table 1). The second version of the paradigm also lasted 5 min and included an initial 30 s period of rest followed by five 15 s stimulus-on periods alternating with four 45 s and followed by a final 15 s stimulus-off periods to complete the 5 min run (protocol n. 2; applied to patients P2, P3, P7, P11, P12, P18; Figure 2; Table 1). To reduce the discomfort of patients due to a long exam duration, only two functional runs were performed (one during salty stimulus application to the left hemitongue, the other to the right); application of the neutral stimulus (water) was omitted, and the activation evoked by salty stimulus was compared with the rest condition.
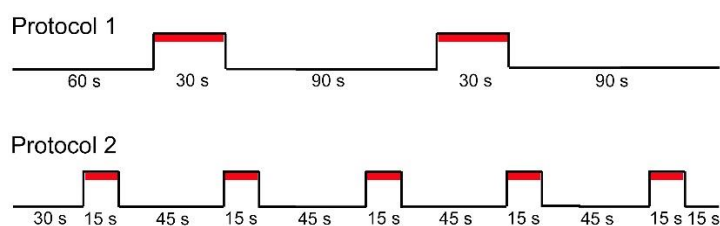

Figure 2. Gustatory stimulation protocols used in the present study. Both protocols were on–off block-designed stimulation paradigm lasting 5 min. The first version (Protocol 1, top track) was composed of an initial 60 s rest, followed by two 30 s stimulus-on periods (red tracks), each followed by 90 s rest periods. The second version (Protocol 2, bottom track) included an initial 30 s period of rest followed by five 15 s stimulus-on periods (red tracks) interleaved with four 45 s rest periods, with a final 15 s stimulus-off period to complete the 5 min run.

2.4. Data Analysis

Functional MRI. After the acquisition session, the images were uploaded into a Unix workstation (General Electric Advantage Windows 4.2) and then to a personal computer. Data were analyzed with the BrainVoyager QX software (BV QX; Version 2.3.1.1770, 32-bit, Copyright© 2001-2023 Rainer Goebel, Brain Innovation, Maastricht, The Netherlands).

The first two images of each functional series were discarded since they were acquired in the period of signal intensity variation because of progressive saturation. Data from all subjects were submitted to pre-processing, which included 3D motion correction. The functional images were overlaid on 2D anatomical images and co-registered into their own 3D data sets by means of trilinear interpolation. Data were then transformed into Talairach space [38].

Statistical analysis was performed using the general linear model (GLM), which predicts the variation of a dependent variable (the fMRI time course) in terms of linear combination. To respect the hemodynamic delay, the predictor time course was convolved with a standard hemodynamic response function (HRF).

The gustatory areas were identified according to standard anatomical landmarks and a reference atlas [39]. In the activated cortical areas, regions of interest (ROIs) were selected, in which the signal increase was analyzed: when it temporally correlated with the stimulus pattern ($p < 0.05$) and was significantly different from the baseline, activation was assumed to be due to the tongue stimulation.

DTI data analysis. The acquired images were transferred to a Unix workstation for post-processing with Functool 3.1.22 (General Electric Medical Systems). EPI distortion was automatically corrected. Diffusion eigenvectors and eigenvalues were calculated from the diffusion tensor and represented the main direction of diffusion and the associated diffusivity. By using orientation-independent fractional anisotropy (FA), anisotropy was calculated. The Functool FiberTrak option allows for the creation of 2D color orientation maps, 2D color eigenvector maps and 3D tractography maps. The 3D volume viewer enables areas of high FA to be displayed as 3D images. The 3D volume viewer allows for the display of the depiction of areas with high fractional anisotropy in 3 dimensions. The viewer is interactive and can be manipulated to view different orientations. The anisotropy threshold for termination of tracking was 0.18, which is above the typical maximum value of gray matter (0.15) and corresponds to a maximum step size of 160 μm.

ROIs were selected in cerebral regions, including activated cortical areas, to track the nerve fibers arising from individual ROIs. ROIs selected in gustatory cortex had 330 mm^2 size. All ROIs were defined manually on color-coded maps of the main diffusion directions.

Statistical analysis. By the Lilliefors test, the age distribution of the two groups was tested: it was normal for patients and not normal for controls.

Because of the small numbers of subjects in both groups (8 patients and 11 healthy volunteers; data from [24]), all comparisons of the activation foci coordinates, the number of activated voxels and the signal increases have been calculated with non-parametric test, i.e., the Wilcoxon. Consequently, the medians and percentiles were reported in all tables in addition to means and standard deviations (Tables 2 and 3). The coordinates comparison was carried out in two steps: in the first step, the three coordinates were analyzed separately (x of patients versus x of controls, y of patients versus y of controls and z of patients versus z of controls); the *p* values thus obtained have been defined as separated. In the second step, to verify whether the position of activation foci could be similar despite significant difference of a single coordinate, the Kruskal–Wallis was used and applied to all coordinates of activation foci. The three coordinates were analyzed as a whole (x, y and z of patients versus x, y and z of controls); the *p* value thus obtained has been defined as global.

To compare activation parameters (coordinates, voxel number and signal increase) in each hemisphere after stimulation of left or right side of the tongue in the same patients, the Wilcoxon test for paired data was applied.

Table 2. Talairach coordinates (x, y, z) of the activation foci evoked in GI area (AIFO) in the 8 callosotomized patients.

| | Left hemitongue Stimulation | | | | | | | | | | Right Hemitongue Stimulation | | | | | | | | | |
| | Ipsilateral AIFO | | | | | Contralateral AIFO | | | | | Ipsilateral AIFO | | | | | Contralateral AIFO | | | | |
Patients	x	y	z	Voxel	%	x	y	z	Voxel	%	x	y	z	Voxel	%	x	y	z	Voxel	%
P2	−28	16	13	351	0.95	37	11	12	37	0.57	41	11	1	362	1.35	−39	11	4	453	0.70
P3	−34	8	15	511	0.30	33	17	18	403	0.44	37	16	7	182	0.33	−28	12	7	391	1.09
P5	−30	16	−1	841	5.23	42	16	−1	769	1.98	36	13	9	696	0.35	−32	11	9	827	0.66
P7	−39	17	7	91	0.51	42	16	9	89	0.89	34	15	7	457	0.84	−31	22	7	90	0.62
P9	−38	18	9	362	0.65	29	20	11	147	0.48	41	17	11	210	0.39	−36	19	11	439	0.34
P11	−35	11	17	70	1.12	30	12	17	128	0.47	40	4	3	148	0.24	−35	4	3	197	0.93
P12	−37	16	362	100	1.42	29	20	11	111	1.31	31	23	12	335	1.69	−32	21	12	318	2.2
P18											31	20	13	181	0.57	−28	9	12	51	0.3
Median	−35	16	13	351	0.95	33	16	11	128	0.57	37	16	8	273	0.48	−32	12	8	355	0.68
25th percentile	−38	14	8	96	0.58	30	14	10	100	0.48	33	13	6	182	0.35	−35	11	6	170	0.55
75th percentile	−32	17	16	437	1.27	40	19	15	275	1.10	40	18	11	386	0.97	−30	20	11	443	0.97
Mean	−34	15	9	332	1.45	35	16	11	241	0.88	36	15	8	321	0.72	−33	14	8	346	0.86
SD	4	4	6	281	1.71	6	4	6	261	0.58	4	6	4	186	0.53	4	6	3	248	0.60

Table 3. Talairach coordinates (x, y, z) of the activation foci evoked in SI area in the 8 callosotomized patients.

| | Left Hemitongue Stimulation | | | | | | | | | | Right Hemitongue Stimulation | | | | | | | | | |
| | Ipsilateral SI | | | | | Contralateral SI | | | | | Ipsilateral SI | | | | | Contralateral SI | | | | |
Patients	x	y	z	Voxel	%	x	y	z	Voxel	%	x	y	z	Voxel	%	x	y	z	Voxel	%
P2	−50	−15	23	156	1.5	55	−16	30	385	0.99	56	−10	34	63	11.92	−46	−10	38	134	0.98
P3	−48	−28	31	149	0.56	52	−30	31	542	0.3	47	−10	30	248	0.25	−42	−15	30	282	0.3
P5																				
P7	−48	−25	33	95	0.33	46	−28	40	516	0.18	51	−27	40	176	0.25	−58	−19	40	637	1.03
P9						56	−10	28	255	0.58										
P11	−53	−23	30	231	0.95	49	−32	28	267	0.76	46	−27	37	132	0.33	−51	−23	37	595	0.41
P12						50	−11	33	43	0.55	45	−29	32	441	0.39	−52	−13	23	861	0.69
P18																−55	−23	38	400	0.4
Median	−49	−24	31	153	0.76	51	−22	31	326	0.57	47	−27	34	176	0.33	−52	−17	38	498	0.55
25th percentile	−51	−26	28	136	0.50	49	−30	29	258	0.36	46	−27	32	132	0.25	−54	−22	32	312	0.40
75th percentile	−48	−21	32	175	1.09	54	−12	33	483	0.72	51	−10	37	248	0.39	−47	−14	38	627	0.91
Mean	−50	−23	29	158	0.84	51	−20	31	335	0.56	49	−21	35	212	2.63	−51	−17	35	485	0.64
SD	2	6	4	56	0.51	4	12	5	187	0.30	5	10	4	145	5.19	6	5	7	263.9	0.32

3. Results

The description of the results will only concern the activations of cortical areas supposed to receive the thalamic inputs from the tongue and convey tactile and taste information to the cortex. These areas correspond to the anterior and middle insula and the frontal and parietal opercula. Further activations eventually observed in other cortical areas, likely belonging to higher-order stages of information processing, are outside the focus of our study. The left-handed participant was included since his individual data were in line with those of the other participants.

3.1. Functional MRI Results

In all patients, salty stimulation applied to either side of the tongue evoked bilateral activation of a cortical region corresponding to the AI and the overlying FO (AIFO; [27,28]). The mean Talairach coordinates (x, y, z; [38]) of the ipsilateral and contralateral foci were, respectively, −34, 15, 9 and 35, 16, 11 for the left hemitongue stimulation; for the right hemitongue stimulation, the mean values were 36, 15, 8 and −33, 14, 8 for the ipsilateral and contralateral foci, respectively (Table 2). Left hemitongue stimulation usually evoked greater activation in the ipsilateral hemisphere (Figure 3A,B), as shown by the number of activated unitary volumes (voxels) and percent of the signal increase (Table 2). Right hemitongue stimulation produces slightly more activation in ipsilateral AIFO in some cases (Figure 3C,D) and in contralateral in others (Figure 3E,F); the mean values of activated voxels and percent of signal increase seem to indicate a slight prevalence in the contralateral hemisphere (Table 2). However, in all cases, the difference did not reach statistical significance (Wilcoxon test $p \geq 0.05$).

Salty stimulation of either side of the tongue also evoked activation in both hemispheres in a region of the parietal cortex corresponding to the tactile tongue representation in the SI area (Figure 4; Table 3). Such activation was generally greater contralateral to the side of stimulation, as shown by the number of activated volumes and percent of the signal increase (Table 3), but the difference was not statistically significant (Wilcoxon test $p \geq 0.05$).

The x, y and z Talairach coordinates of the activation foci evoked in the eight patients were compared with those obtained in previous studies from 11 healthy volunteers submitted to the same stimulation protocol [24] once age difference was verified as not statistically significant ($p = 0.0937$, non-paired Wilcoxon Test). The analysis was carried out in two steps; in the first step, the Wilcoxon test for non-paired-data was applied to three coordinates that were analyzed separately (x of patients versus x of controls, y of patients versus y of controls and z of patients versus z of controls); in the second step, the three coordinates were analyzed as a whole (x, y and z of patients versus x, y and z of controls). After the first analysis, with a separated modality (see Section 2), the results generally did not show any differences between the two groups ($p > 0.05$), except for the x and z coordinates of activation foci in the GI area of the left hemisphere in both conditions (left and right tongue stimulation) and z coordinate in the right, after left side stimulation. In the SI area, the coordinates of activation foci did not significantly differ from those previously reported in healthy subjects, except for the z value in the right SI in both conditions (left and right tongue stimulation). To verify whether the cortical location of the activation foci could be considered similar despite the significant difference of a single coordinate, the Kruskal–Wallis test was used. In this analysis, with the global modality, the results did not show any differences between the two groups ($p > 0.05$; Table 4).
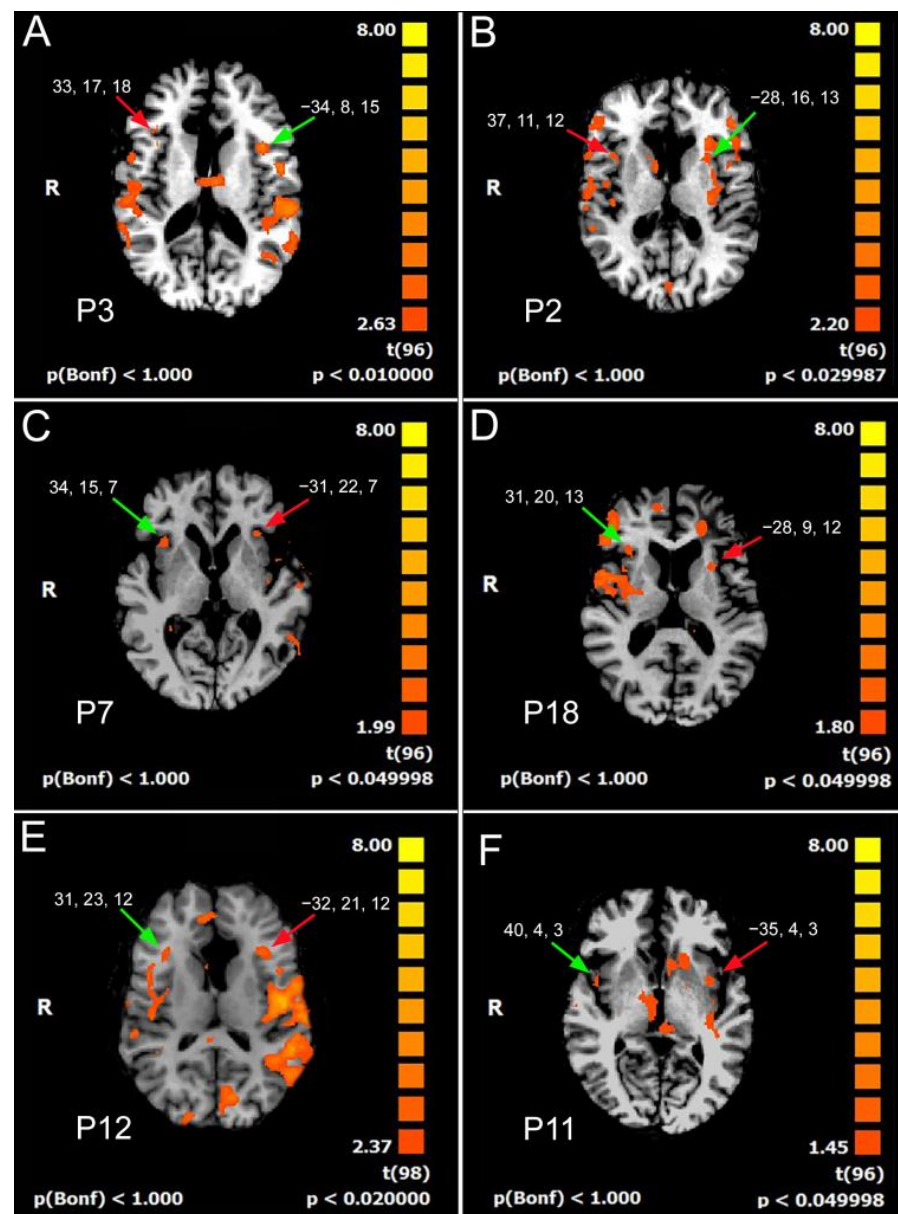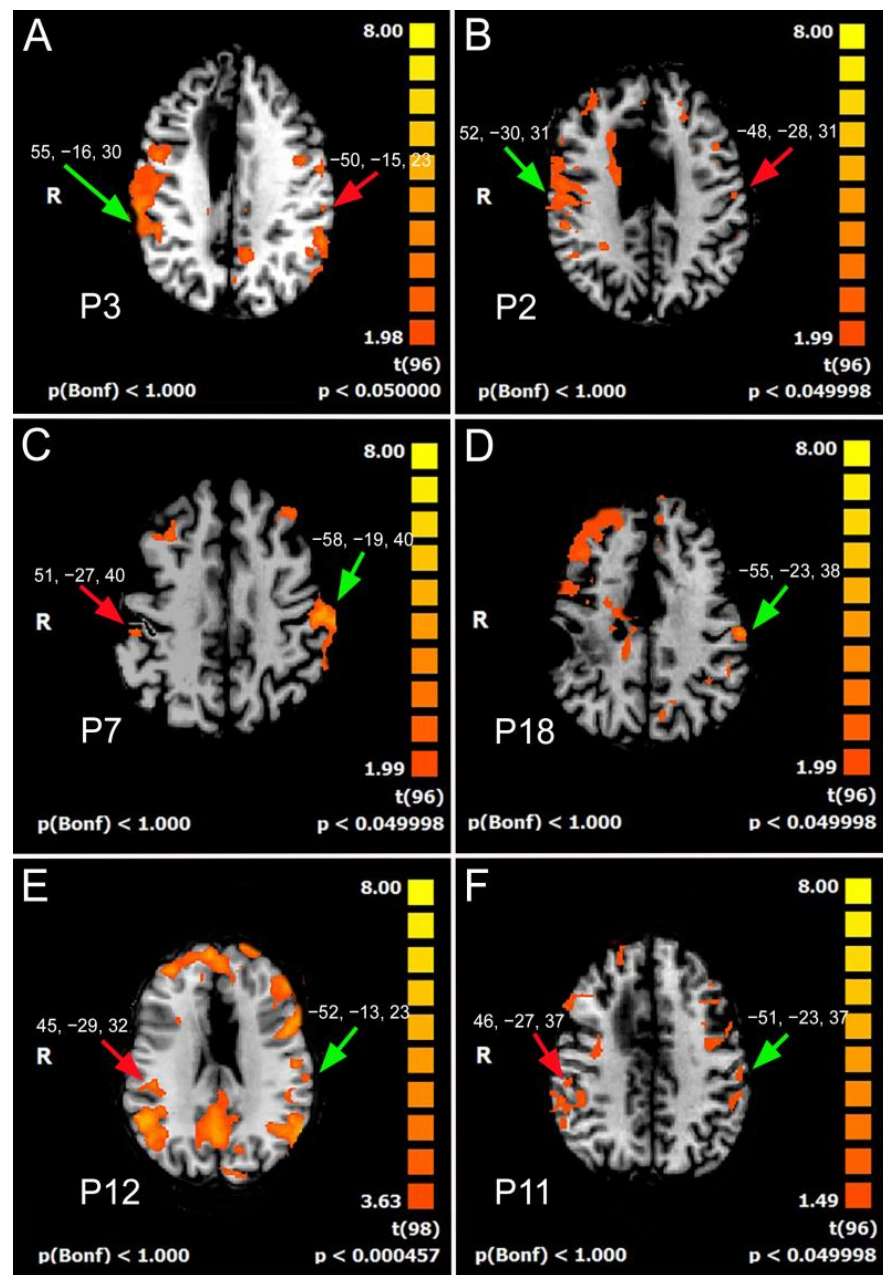
Figure 3. Bilateral activation of GI area. (**A**,**B**) Salty stimulation of the left tongue in patients P3 and P2, respectively, both with total callosotomy. (**C**) Salty stimulation of right tongue in patient P7, with partial posterior resection. (**D**) Salty stimulation of right tongue in patient P18, with central callosotomy. (**E**,**F**) Salty stimulation of right tongue in patients P12 and P11, respectively, both with partial anterior resection. Green arrows, ipsilateral GI activation; red arrows, contralateral GI activation. R, right. Left hemisphere is shown on the right, according to the radiological convention.

Figure 4. Bilateral activation of SI area. (**A**,**B**) Salty stimulation of the left tongue in patients P3 and P2, respectively, both with total callosotomy. (**C**) Salty stimulation of right tongue in patient P7, with partial posterior resection. (**D**) Salty stimulation of right tongue in patient P18, with central callosotomy. (**E**,**F**) Salty stimulation of right tongue in patients P12 and P11, respectively, both with partial anterior resection. Green arrows, contralateral SI activation; red arrows, ipsilateral SI activation. R, right. Left hemisphere is shown on the right, according to the radiological convention.
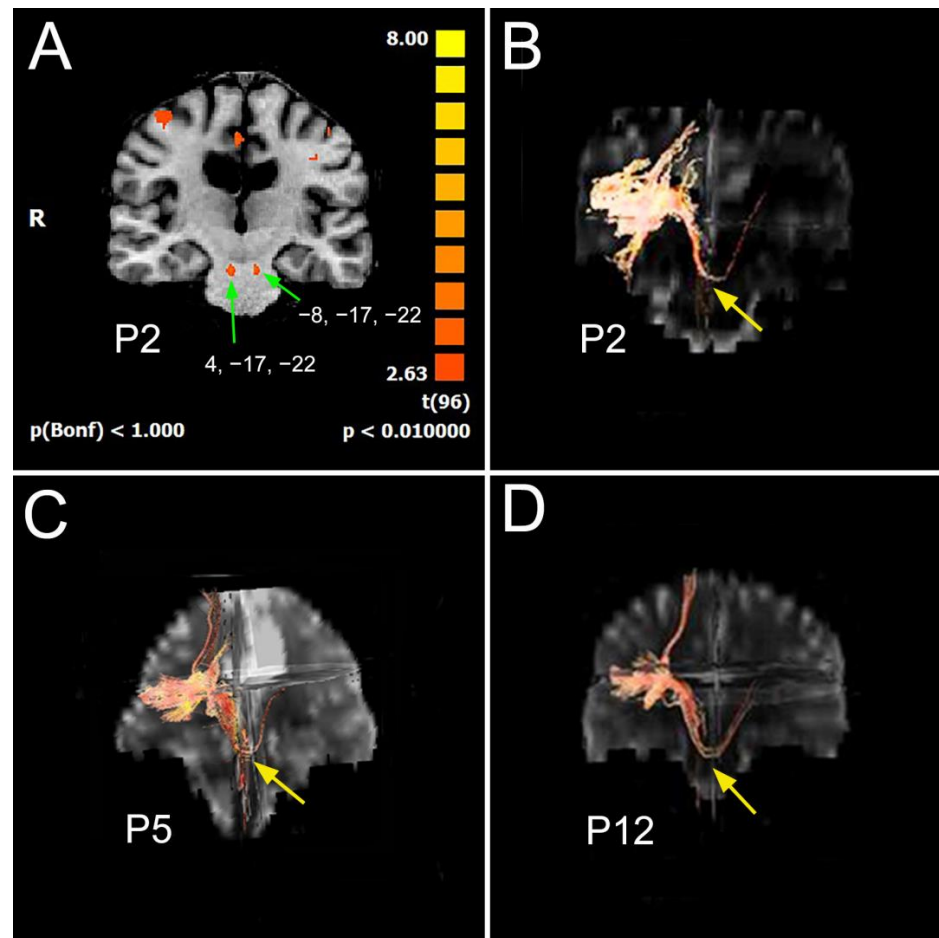
Figure 5. (**A**) Activation in the PBN on both sides in patient P2 after salty stimulation of the right hemitongue. (**B**) In the same patient (P2), fibers from right GI area connect to ipsilateral PBN (yellow arrow), cross the midline toward the contralateral PBN and then connect to contralateral GI. (**C,D**) Similar pathways connecting GI areas in the two hemispheres are observed in another totally callosomized patient, P5, and in a patient with anterior callosotomy, P12, in whom the callosal fibers between GI areas are interrupted. Green arrows indicate the activation in bilateral PBN; yellow arrows indicate the fiber bundle crossing the midline at pontine level. R, right. Left hemisphere is shown on the right, according to the radiological convention.

Table 4. Paired t test applied to the mean Talairach coordinates (x, y, z) of the activation foci evoked in GI (A) and SI (B) areas in the 8 patients and in 11 healthy volunteers (from [24]).

A	Left Hemitongue Stimulation										Right Hemitongue Stimulation									
	Ipsilateral AIFO					Contralateral AIFO					Ipsilateral AIFO					Contralateral AIFO				
	x	y	z	Voxel	%	x	y	z	Voxel	%	x	y	z	Voxel	%	x	y	z	Voxel	%
Patients																				
Median	−35	16	13	351	0.95	33	16	11	128	0.57	37	16	8	273	0.48	−32	12	8	355	0.68
25th percentile	−38	14	8	96	0.58	30	14	10	100	0.48	33	13	6	182	0.35	−35	11	6	170	0.55
75th percentile	−32	17	16	437	1.27	40	19	15	275	1.10	40	18	11	386	0.97	−30	20	11	443	0.97
Controls																				
Median	−45	14	4	251	2	37	12	4	135	1.00	38	16	4	165	1	−39	16	4	147	2.00
25th percentile	−46	7	0	139	1	35	6	1	104	0.90	35	14	1	60	1	−48	15	1	90	1.00
75th percentile	−40	21	4	940	2	45	16	4	432	2.00	45	20	8	294	4	−36	19	7	362	4.30
Wilcoxon non-paired data	0.001	0.68	0.56	0.92	0.07	0.17	0.26	0.009	0.84	0.01	0.26	0.84	0.16	0.32	0.02	0.02	0.21	0.04	0.44	0.01
Kruskal–Wallis test		0.13					0.33					0.92					0.62			
B	Left Hemitongue Stimulation										Right Hemitongue Stimulation									
	Ipsilateral SI					Contralateral SI					Ipsilateral SI					Contralateral SI				
	x	y	z	Voxel	%	x	y	z	Voxel	%	x	y	z	Voxel	%	x	y	z	Voxel	%
Patients																				
Median	−49	−24	31	153	0.76	51	−22	31	326	0.57	47	−27	34	176	0.33	−52	−17	38	498	0.55
25th percentile	−51	−26	28	136	0.50	49	−30	29	258	0.36	46	−27	32	132	0.25	−54	−22	32	312	0.40
75th percentile	−48	−21	32	175	1.09	54	−12	33	483	0.72	51	−10	37	248	0.39	−47	−14	38	627	0.91
Controls																				
Median	−55	−18.5	25.5	478,5	0.8	51.5	−16.5	25.5	510	0.7	54	−18	23	340	0.6	−55	−19	29	568	0.9
25th percentile	−57	−21.5	24	300	0.7	48	−20	22	400.5	0.6	52	−18.5	21.5	159.5	0.5	−57	−20	26	180	0.8
75th percentile	−52	−16.5	26.5	723.5	1.4	54.5	−11.5	29	767	0.9	55.5	−15.5	27	382	1	−50	−18	31	614	1.2
Wilcoxon non-paired data	0.12	0.24	0.11	0.07	0.57	0.94	0.39	0.09	0.14	0.30	0.22	0.43	0.01	0.64	0.32	0.46	0.55	0.14	0.66	0.13
Kruskal–Wallis test		0.67					0.89					0.91					0.54			

In all patients studied, activation foci elicited by salty stimuli to the left or right hemitongue were also found bilaterally in the thalamic ventropostero-medial nucleus (VPMpc; not shown), and also in the pontine PBN of both sides in patient P2 (Figure 5). Activation in the VPMpc and PBN was observed in some of the healthy subjects previously studied [24]. The lack of pontine activation foci in most patients and control subjects is likely due to the selection of brain tissue to scan during the acquisition step (see Section 4).

3.2. DTI Results

Analyzing the diffusion of water molecules along different directions, DTI enables the virtual reconstruction of axonal fibers. Tractography was applied to all patients. ROIs were placed in the GI area according to the activation foci evoked by salty stimulation during fMRI in each subject.

Diffusion tensor tractography (DTT) in a patient with posterior CC resection showed that the fibers interconnecting the GI of the two hemispheres cross the anterior CC, as previously observed in healthy subjects [40,41]. In patients with anterior and total resection, DTT showed that fibers from the GI area seem to reach a pontine structure, likely the parabrachial nucleus (PBN; Figure 5), and from here, fibers seem to go up toward the cortex in the contralateral hemisphere. Since a pathway as that observed, i.e., connecting the GI areas of the two hemispheres by a fiber tract crossing at the pontine level, has never been described, this picture seems to suggest a branching at the pontine level of different bundles rather than a bending of a single fiber tract (see Section 4).

4. Discussion

The present study reports fMRI findings obtained in totally and partially callosotomized patients, to whom salty stimulation was applied to either side of the tongue in separate scan sessions. In all patients, bilateral activation of the GI area in the anterior insula-frontal operculum was observed, and in most of them, bilateral activation of the SI area in the parietal lobe was also observed. The mean Talairach coordinates of the contralateral and ipsilateral activation foci evoked in the GI area by salty stimulation of the left and right side of the tongue in callosotomized patients were not significantly different in the two hemispheres (nor from the corresponding values observed in similar stimulation conditions in control subjects ($p > 0.05$; Table 2)) reported in a previous fMRI study [24].

These results confirm previous studies on healthy subjects and on patients with brain lesions in different sites, performed with many different techniques, and more recent neuropsychological findings collected in split-brain patients, indicating that gustatory projections from tongue to cortex are bilaterally distributed, with an ipsilateral predominance.

In addition, the present results demonstrate that CC is not the sole path allowing the taste information from one side of the tongue to reach the GI area in the contralateral hemisphere.

There is a general agreement that gustatory stimuli reach the ipsilateral GI area via the NST in the medulla, then project to ipsilateral GI via the thalamic VPMpc and to contralateral GI through the CC. In subjects with an intact brain, bilateral GI activation appears to be thus supported by the anterior portion of the CC. The bilateral activation of the GI area detected in patients lacking the anterior part of CC suggests the existence of an additional extracallosal pathway that could subserve the bilateral representation of taste in the brain. The existence of a direct subcortical pathway responsible for the bilateral activation of GI areas was also suggested by latency measures, as previously shown by Onoda and coworkers [16]. In their study, these authors reported that the difference in average latencies of GI area responses between the two hemispheres was 3 ms, considerably lower than the CC conduction times of the other sensory systems. Furthermore, the difference between the average latencies of GI activation of the two hemispheres was not statistically significant [16].

Many hypotheses can be advanced to explain the origin of the extracallosal pathway, as suggested in the models previously proposed [18,23]. In an fMRI study, Iannilli et al. [20] recorded the brain activity evoked by applying salty and umami taste to both sides of the

tongue and found ipsilateral activation up to the thalamic level; they, therefore, hypothesized that the branching point of taste pathways be above thalamus. By examining the clinical findings of patients with taste disorders due to central lesions in the same year, Onoda et al. [17] suggested that the taste pathways conveying information bilaterally to the GI area branches at the pons level, likely projecting to the PBN of both sides, which in turn project to the thalamic nuclei of both hemispheres and then to GI areas.

However, this pontine nucleus, which is an intermediate station in the taste pathways of many mammalian species [23], does not seem to be involved in taste in primates, including humans [42], in that the NST projections bypass the PBN and directly project to the VPMpc [43,44]. In subprimate species, the caudal and ventral portions of the medial PBN (waist area) receive afferents from the rostral and, to a lesser extent, the caudal NST [45]. The rostral NST-PBN projections are mostly ipsilateral, although, in rats and mice, the caudal NST-PBN afferents are also found to terminate in the contralateral PBN [46,47]; in addition, after unilateral injection of a retrograde tracer in the PBN, a small number of retrogradely labeled neurons were found in contralateral PBN in mouse [47].

The PBN then strongly projects to the thalamic nucleus VPMpc, anterior to the gustatory part of the nucleus [48], and to the insular cortex [49]. These data are consistent with previous neurophysiological [50] and behavioral [51] data demonstrating that in the monkey, the gustatory region of VPMpc is restricted to the posterior half of the nucleus. Also, in other species (squirrel monkeys [52] and cats [53]), electrical stimulation of the chorda tympani and glossopharyngeal nerves activates neurons within the posterior half of VPMpc but not the anterior [43].

Other than being involved in the gustatory pathway, at least in rodents [42], the lateral PBN is a component of a distributed network that controls sodium and water balance and, thereby, extracellular fluid volume and blood pressure [54,55], thirst [56], sodium appetite [57,58] and hunger [59–63].

In the present research, bilateral activation of pontine PBN was observed only in one patient carrying total callosotomy (P2). In other patients, the fMRI images were not acquired from the dorso-ventral level in which the PBN is located; therefore, it was not possible to verify whether there is an activation of this pontine nucleus.

The activation of PBN was never reported in previous functional studies on humans. The reason could reside in the level of acquired images, as in the case of most patients considered in the present study. Another explanation, which is related to the role pf PBN in the regulation of salt intake, could be that the concentration of salty stimulus in the present study (NaCl 1M) is higher than in previous studies (50 mM and 200 mM in [20] and [12], respectively), likely provoking a stronger activation that is more easily detectable.

By analyzing the DTT results, a pathway from the GI of one hemisphere to the pons and then to the contralateral GI is tracked. It is known that such a bundle does not exist in mammals, but the observed picture could be the result of the technical limits of DTI tractography, which cannot distinguish between a curved fibers bundle and crossing or branching fibers [64–66]. This result can, therefore, be interpreted as being due to branching fibers from PBN to the thalamus or to fibers arising from NTS and crossing at the PBN level.

Putting these observations together, i.e., the bilateral activation of PBN and the pathway from GI to the contralateral side through the pons, two new models can be proposed (Figure 6), which both derive from that suggested by Onoda and coworkers [17] and are consistent with their observation of one case with a contralateral taste disorder caused by a medullary lesion and two cases with a pontine lesion provoking a bilateral or contralateral taste disorder [17]. According to the first model, gustatory fibers from each hemitongue project to ipsilateral NST, which in turn projects to the ipsilateral PBN; from here, some fibers go towards the thalamic VPMpc of the same side, and other fibers cross the midline to the contralateral PBN and VPMpc (Figure 6A); according to the second model, gustatory fibers from each hemitongue project bilaterally to NST, although more heavily to the ipsilateral side, and each NST in turn projects to the ipsilateral PBN, and then to the thalamic

VPMpc of the same side (Figure 6B). As a result, in both cases, the gustatory information is conveyed to the GI areas of both hemispheres.
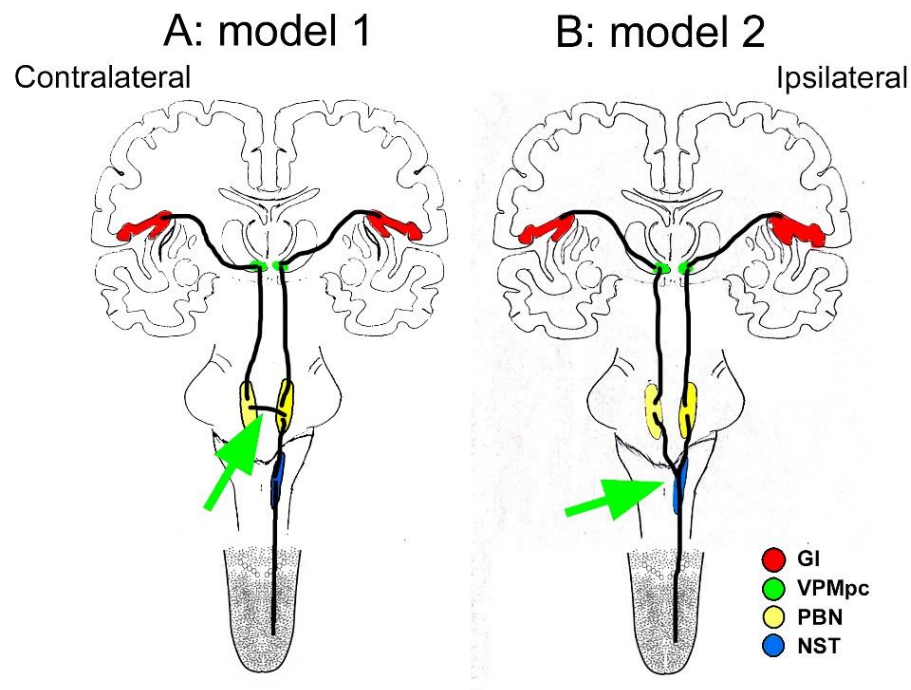

Figure 6. Model of possible pathways explaining the bilateral activation of GI area, as well as in absence of the CC: the crossing point has been hypothesized at pontine level (**A**, arrow) or at medulla level (**B**, arrow). GI, primary gustatory area; NTS, nucleus of solitary tract; PBN, parabrachialis nucleus; VPMpc, ventroposteromedial nucleus, parvicellular portion.

In conclusion, the activation of the GI area in both hemispheres observed in callosotomized patients suggests that the CC does play a role in the bilateral representation of gustatory sensitivity in the GI area, but it is not the sole pathway underpinning the transfer of gustatory information to contralateral GI. The bilateral response observed in GI leads to hypothesizing two different gustatory pathways from NST, where the chorda tympani and glossopharyngeal nerves terminate: one pathway diverges at NST or pontine level and terminates at the GI area in both hemispheres via the bilateral thalamic relay; the other pathway via ipsilateral NST and VPMpc, which terminates at the ipsilateral GI and then leads to its counterpart in the other hemisphere via the CC. In this view, the callosal connections between the GI areas of the two sides probably have a modulatory function balancing the differential effects of the ipsilateral and contralateral pathway, activating similar volumes with similar signal intensity in cortical GI areas of the two hemispheres, thus making the information reaching the two GI areas symmetrical in both sides of the brain. Further studies will be necessary to elucidate whether the PBN is also part of gustatory pathways in humans and where the bifurcating point is along the ascending bundles.

The small number of patients, which is the major limitation of this study, is, however, justified by the fact that there are rather few patients who have undergone callosotomy. In addition, this type of operation, carried out in the past to treat drug-resistant epilepsy, is at present performed ever less frequently.

Author Contributions: Conceptualization, M.F. and G.P.; methodology, M.F., G.M. and G.P.; software, G.M. and G.P.; validation, U.S., A.P. and T.M.; formal analysis, G.M. and M.F.; investigation, G.P., G.M. and M.F.; resources, A.P. and G.P.; data curation, A.P.; writing—original draft preparation, M.F. and G.M.; writing—review and editing, M.F. and G.P.; visualization, G.M., G.P. and M.F.; supervision, T.M. and U.S.; project administration, M.F. and G.P.; funding acquisition, M.F. and T.M. All authors have read and agreed to the published version of the manuscript.

Informed Consent Statement: Informed consent was obtained from all subjects involved in the study.

Data Availability Statement: Data were obtained from Azienda Ospedaliera-Universitaria Umberto I and are available from the authors with the permission of Azienda Ospedaliera-Universitaria Umberto I.

Conflicts of Interest: The authors declare no conflict of interest.

References

1. Pritchard, T.C. Gustatory system. In *The Human Nervous System*, 3rd ed.; Mai, J.K., Paxinos, G., Eds.; Elsevier: Oxford, UK, 2012; pp. 1187–1218.
2. Rolls, E.T. Taste, olfactory, and food reward value processing in the brain. *Prog. Neurobiol.* **2015**, *127–128*, 64–90. [CrossRef] [PubMed]
3. Disbrow, E.A.; Hinkley, L.B.; Roberts, T.P. Ipsilateral representation of oral structures in human anterior parietal somatosensory cortex and integration of inputs across the midline. *J. Comp. Neurol.* **2003**, *467*, 487–495. [CrossRef] [PubMed]
4. Tamura, Y.; Shibukawa, Y.; Shintani, M.; Kaneko, Y.; Ichinohe, T. Oral structure representation in human somatosensory cortex. *Neuroimage* **2008**, *43*, 128–135. [CrossRef] [PubMed]
5. Sakamoto, K.; Nakata, H.; Yumoto, M.; Kakigi, R. Somatosensory processing of the tongue in humans. *Front. Physiol.* **2010**, *1*, 136. [CrossRef] [PubMed]
6. Boling, W.; Reutens, D.C.; Olivier, A. Functional topography of the low postcentral area. *J. Neurosurg.* **2002**, *97*, 388–395. [CrossRef] [PubMed]
7. Maezawa, H.; Mima, T.; Yazawa, S.; Matsuhashi, M.; Shiraishi, H.; Hirai, Y.; Funahashi, M. Contralateral dominance of corticomuscular coherence for both sides of the tongue during human tongue protrusion: An MEG study. *Neuroimage* **2014**, *101*, 245–255. [CrossRef] [PubMed]
8. Frey, S.; Petrides, M. Re-examination of the human taste region: A positron emission tomography study. *Eur. J. Neurosci.* **1999**, *11*, 2985–2988. [CrossRef]
9. Small, D.M.; Zald, D.H.; Jones-Gotman, M.; Zatorre, R.J.; Pardo, J.V.; Frey, S.; Petrides, M. Human cortical gustatory areas: A review of functional neuroimaging data. *Neuroreport* **1999**, *10*, 7–14. [CrossRef]
10. Nakamura, Y.; Goto, T.K.; Tokumori, K.; Yoshiura, T.; Kobayashi, K.; Nakamura, Y.; Honda, H.; Ninomiya, Y.; Yoshiura, K. Localization of brain activation by umami taste in humans. *Brain Res.* **2011**, *1406*, 18–29. [CrossRef]
11. Nakamura, Y.; Tokumori, K.; Tanabe, H.C.; Yoshiura, T.; Kobayashi, K.; Nakamura, Y.; Honda, H.; Yoshiura, K.; Goto, T.K. Localization of the primary taste cortex by contrasting passive and attentive conditions. *Exp. Brain Res.* **2013**, *227*, 185–197. [CrossRef]
12. Iannilli, E.; Noennig, N.; Hummel, T.; Schoenfeld, A.M. Spatio-temporal correlates of taste processing in the human primary gustatory cortex. *Neuroscience* **2014**, *273*, 92–99. [CrossRef] [PubMed]
13. Pardo, J.V.; Wood, T.D.; Costello, P.A.; Pardo, P.J.; Lee, J.T. PET study of the localization and laterality of lingual somatosensory processing in humans. *Neurosci. Lett.* **1997**, *234*, 23–26. [CrossRef] [PubMed]
14. Aglioti, S.; Tassinari, G.; Corballis, M.C.; Berlucchi, G. Incomplete gustatory lateralization as shown by analysis of taste discrimination after callosotomy. *J. Cogn. Neurosci.* **2000**, *12*, 238–245. [CrossRef] [PubMed]
15. Aglioti, S.M.; Tassinari, G.; Fabri, M.; Del Pesce, M.; Quattrini, A.; Manzoni, T.; Berlucchi, G. Taste laterality in the split brain. *Eur. J. Neurosci.* **2001**, *13*, 195–200. [CrossRef] [PubMed]
16. Onoda, K.; Kobayakawa, T.; Ikeda, M.; Saito, S.; Kida, A. Laterality of human primary gustatory cortex studied by MEG. *Chem. Senses* **2005**, *30*, 657–666. [CrossRef] [PubMed]
17. Onoda, K.; Ikeda, M.; Sekine, H.; Ogawa, H. Clinical study of central taste disorders and discussion of the central gustatory pathway. *J. Neurol.* **2012**, *259*, 261–266. [CrossRef] [PubMed]

18. Stevenson, R.J.; Miller, L.A.; McGrillen, K. The lateralization of gustatory function and the flow of information from tongue to cortex. *Neuropsychologia* **2013**, *51*, 1408–1416. [CrossRef] [PubMed]

19. Berlucchi, G.; Moro, V.; Guerrini, C.; Aglioti, S.M. Dissociation between taste and tactile extinction on the tongue after right brain damage. *Neuropsychologia* **2004**, *42*, 1007–1016. [CrossRef]

20. Iannilli, E.; Singh, P.B.; Schuster, B.; Gerber, J.; Hummel, T. Taste laterality studied by means of umami and salt stimuli: An fMRI study. *Neuroimage* **2012**, *60*, 426–435. [CrossRef]

21. Lee, B.; Hwang, S.; Rison, R.; Chang, G. Central pathway of taste: Clinical and MRI study. *Eur. Neurol.* **1998**, *39*, 200–203. [CrossRef]

22. Pritchard, T.C.; Macaluso, D.A.; Eslinger, P.J. Taste perception in patients with insular cortex lesions. *Behav. Neurosci.* **1999**, *113*, 663–671. [CrossRef]

23. Iannilli, E.; Gudziol, V. Gustatory pathway in humans: A review of models of taste perception and their potential lateralization. *J. Neurosci. Res.* **2018**, *97*, 230–240. [CrossRef] [PubMed]

24. Mascioli, G.; Berlucchi, G.; Pierpaoli, C.; Salvolini, U.; Barbaresi, P.; Fabri, M.; Polonara, G. Functional MRI cortical activations from unilateral tactile-taste stimulations of the tongue. *Physiol. Behav.* **2015**, *151*, 221–229. [CrossRef] [PubMed]

25. Landis, B.N.; Welge-Luessen, A.; Brämerson, A.; Bende, M.; Mueller, C.A.; Nordin, S.; Hummel, T. "Taste strips"—A rapid, lateralized, gustatory bedside identification test based on impregnated filter papers. *J. Neurol.* **2009**, *256*, 242–248. [CrossRef] [PubMed]

26. Faurion, A.; Kobayakawa, T.; Cerf-Ducastel, B. Functional magnetic resonance imaging study of taste. In *The Senses*; Firesten, S., Beauchamp, G.K., Eds.; Olfaction and Taste; Elsevier: Oxford, UK, 2008; Volume 4, pp. 271–279.

27. Veldhuizen, M.G.; Albrecht, J.; Zelano, C.; Boesveldt, S.; Breslin, P.; Lundström, J.N. Identification of human gustatory cortex by activation likelihood estimation. *Hum. Brain Mapp.* **2011**, *32*, 2256–2266. [CrossRef] [PubMed]

28. Small, D.M. Taste representation in the human insula. *Brain Struct. Funct.* **2010**, *214*, 551–561. [CrossRef] [PubMed]

29. Penfield, W.; Boldrey, E. Somatic motor and sensory representation in the cerebral cortex of man as studied by electrical stimulation. *Brain* **1937**, *60*, 389–443. [CrossRef]

30. Picard, C.; Olivier, A. Sensory cortical tongue representation in man. *J. Neurosurg.* **1983**, *59*, 781–789. [CrossRef] [PubMed]

31. Polonara, G.; Fabri, M.; Mascioli, G.; Tassinari, G.; Berlucchi, G.; Manzoni, T.; Salvolini, U. The cortical representation of taste in the human brain: An f MRI study. In Proceedings of the European Congress of Radiology (ECR), Vienna, Austria, 3–7 March 2006.

32. Polonara, G.; Mascioli, G.; Paggi, A.; Tassinari, G.; Berlucchi, G.; Salvolini, U.; Manzoni, T.; Fabri, M. The cortical representation of taste in the human brain: An fMRI study on callosotomized patients. In Proceedings of the 12th International Conference on Human Brain Mapping (HBMO), Florence, Italy, 11–15 June 2006.

33. Fabri, M.; Polonara, G. Functional topography of the corpus callosum as revealed by fMRI and behavioural studies of control subjects and patients with callosal resection. *Neuropsychologia* **2023**, *183*, 108533. [CrossRef]

34. Quattrini, A.; Papo, I.; Paggi, A.; Ortensi, A.; Rychlicki, F.; Fronzoni, M.; Recchioni, M.A.; Marchioro, R.; Pauri, G.L.; Bonaparte, A.; et al. Anterior callosotomy in drug-resistant epilepsy. *Adv. Epileptol.* **1989**, *17*, 42–45.

35. Pizzini, F.B.; Polonara, G.; Mascioli, G.; Beltramello, A.; Moroni, R.; Paggi, A.; Salvolini, U.; Tassinari, G.; Fabri, M. Diffusion tensor tracking of callosal fibers several years alter callosotomy. *Brain Res.* **2010**, *1312*, 10–17. [CrossRef]

36. Oldfield, R.C. The assessment and analysis of handedness: The Edinburg inventory. *Neuropsychologia* **1971**, *9*, 97–113. [CrossRef] [PubMed]

37. Kim, S.-G.; Urgubil, K. Functional magnetic resonance imaging of the human brain. *J. Neurosci. Methods* **1997**, *15*, 3821–3839. [CrossRef] [PubMed]

38. Talairach, J.; Turnoux, P. *Co-Planar Stereotaxic Atlas of the Human Brain*; Thieme Medical Publishers: New York, NY, USA, 1988; pp. 1–122.

39. Mai, J.K.; Assheuer, J.; Paxinos, G. *Atlas of the Human Brain*; Academic Press: San Diego, CA, USA, 1997; pp. 1–328.

40. Fabri, M.; Polonara, G. Functional topography of human corpus callosum: An FMRI mapping study. *Neural Plast.* **2013**, *2013*, 251308. [CrossRef] [PubMed]

41. Polonara, G.; Mascioli, G.; Foschi, N.; Salvolini, U.; Pierpaoli, C.; Manzoni, T.; Fabri, M.; Barbaresi, P. Further evidence for the topography and connectivity of the corpus callosum: An fMRI study of patients with partial callosal resection. *J. Neuroimaging* **2015**, *25*, 465–473. [CrossRef] [PubMed]

42. Vincis, R.; Fontanini, A. Central taste anatomy and physiology. *Handb. Clin. Neurol.* **2019**, *164*, 187–204. [PubMed]

43. Pritchard, T.C.; Hamilton, R.B.; Norgren, R. Projections of the Parabrachial Nucleus in the Old World Monkey. *Exp. Neurol.* **2000**, *165*, 101–117. [CrossRef]

44. Simon, S.A.; de Araujo, I.E.; Gutierrez, R.; Nicolelis, M.A. The neural mechanisms of gustation: A distributed processing code. *Nat. Rev. Neurosci.* **2006**, *7*, 890–901. [CrossRef]

45. Herbert, H.; Moga, M.M.; Saper, C.B. Connections of the parabrachial nucleus with the nucleus of the solitary tract and the medullary reticular formation in the rat. *J. Comp. Neurol.* **1990**, *293*, 540–580. [CrossRef]

46. Williams, J.B.; Murphy, D.M.; Reynolds, K.E.; Welch, S.J.; King, M.S. Demonstration of a bilateral projection from the rostral nucleus of the solitary tract to the medial parabrachial nucleus in rat. *Brain Res.* **1996**, *737*, 231–237. [CrossRef]

47. Tokita, K.; Inoue, T.; Boughter, J.D., Jr. Afferent connections of the parabrachial nucleus in C57BL/6J mice. *Neuroscience* **2009**, *161*, 475–488. [CrossRef] [PubMed]

48. Beckstead, R.M.; Morse, J.; Norgren, R. The nucleus of the solitary tract in the monkey: Projections to thalamus and other brainstem nuclei. *J. Comp. Neurol.* **1980**, *90*, 259–282. [CrossRef] [PubMed]

49. Pritchard, T.C.; Hamilton, R.B.; Morse, J.; Norgren, R. Projections of thalamic gustatory and lingual areas in the monkey, Macaca fascicularis. *J. Comp. Neurol.* **1986**, *244*, 213–228. [CrossRef] [PubMed]

50. Pritchard, T.C.; Hamilton, R.B.; Norgren, R. Neural coding of gustatory information in the thalamus of Macaca mulatta. *J. Neurophysiol.* **1989**, *61*, 1–14. [CrossRef] [PubMed]

51. Reilly, S.; Pritchard, T.C. The effect of thalamic lesions on primate taste preference. *Exp. Neurol.* **1995**, *135*, 56–66. [CrossRef] [PubMed]

52. Blomquist, A.J.; Benjamin, R.M.; Emmers, R. Thalamic localization of afferents from the tongue in squirrel monkey (Saimiri sciureus). *J. Comp. Neurol.* **1962**, *118*, 77–88. [CrossRef] [PubMed]

53. Emmers, R. Localization of thalamic projection of afferents from the tongue in the cat. *Anat. Rec.* **1962**, *148*, 67–74. [CrossRef]

54. Menani, J.V.; De Luca, L.A., Jr.; Johnson, A.K. Role of the lateral parabrachial nucleus in the control of sodium appetite. *Am. J. Physiol.-Regul. Integr. Comp. Physiol.* **2014**, *306*, R201–R210. [CrossRef]

55. Benarroch, E.E. Parabrachial nuclear complex: Multiple functions and potential clinical implications. *Neurology* **2016**, *86*, 676–683. [CrossRef]

56. Edwards, G.L.; Johnson, A.K. Enhanced drinking after excitotoxic lesions of the parabrachial nucleus in the rat. *Am. J. Physiol. Regul. Integr. Comp. Physiol.* **1991**, *261*, R1039–R1044. [CrossRef]

57. Menani, J.V.; Thunhorst, R.L.; Johnson, A.K. Lateral parabrachial nucleus and serotonergic mechanisms in the control of salt appetite in rats. *Am. J. Physiol. Regul. Integr. Comp. Physiol.* **1996**, *270*, R162–R168. [CrossRef] [PubMed]

58. Geerling, J.C.; Loewy, A.D. Sodium depletion activates the aldosterone sensitive neurons in the NTS independently of thirst. *Am. J. Physiol. Regul. Integr. Comp. Physiol.* **2007**, *292*, R1338–R1348. [CrossRef] [PubMed]

59. Higgs, S.; Cooper, S.J. Hyperphagia induced by direct administration of midazolam into the parabrachial nucleus of the rat. *Eur. J. Pharmacol.* **1996**, *313*, 1–9. [CrossRef] [PubMed]

60. Wu, Q.; Boyle, M.P.; Palmiter, R.D. Loss of GABAergic signaling by AgRP neurons to the parabrachial nucleus leads to starvation. *Cell* **2009**, *137*, 1225–1234. [CrossRef] [PubMed]

61. Geerling, J.C.; Shin, J.W.; Chimenti, P.C.; Loewy, A.D. Paraventricular hypothalamic nucleus: Axonal projections to the brainstem. *J. Comp. Neurol.* **2010**, *518*, 1460–1499. [CrossRef] [PubMed]

62. Li, M.M.; Madara, J.C.; Steger, J.S.; Krashes, M.J.; Balthasar, N.; Campbell, J.N.; Resch, J.M.; Conley, N.J.; Garfield, A.S.; Lowell, B.B. The paraventricular hypothalamus regulates satiety and prevents obesity via two genetically distinct circuits. *Neuron* **2019**, *102*, 653–667. [CrossRef]

63. Grady, F.; Peltekian, L.; Iverson, G.; Geerling, J.C. Direct parabrachial–cortical connectivity. *Cereb. Cortex* **2020**, *30*, 4811–4833. [CrossRef]

64. Calamante, F. The seven deadly sins of measuring brain structural connectivity using diffusion MRI streamlines fibre-tracking. *Diagnostics* **2019**, *9*, 115. [CrossRef]

65. Dell'Acqua, F.; Tournier, J.D. Modelling white matter with spherical deconvolution: How and why? *NMR Biomed.* **2019**, *32*, e3945. [CrossRef]

66. Jeurissen, B.; Descoteaux, M.; Mori, S.; Leemans, A. Diffusion MRI fiber tractography of the brain. *NMR Biomed.* **2019**, *32*, e3785. [CrossRef]